Achievable Environment Rigidity of a Haptic Display to Guarantee Stability

YangYu Luo, HongLin Liu, ChengRong Li
Institute of Automation,
Chinese Academy of Sciences
Beijing China
yyluo@hitic.ia.ac.cn, hlliu@hitic.ia.ac.cn,
lich@hitic.ia.ac.cn

YuRu Zhang
Department of mechanical engineer,
Beijing University of Aeronautic and Astronautic
Beijing China
yru@buaa.edu.cn

***Abstract*—To study the effect of transmission stiffness on the stability of a haptic display in virtual reality, a one-DOF(degree of freedom) haptic display system is modeled as a two-port electric network, and its absolute stable condition is provided according to two-port stable theory. Stability of a haptic display system can be evaluated by the achievable spring rigidity when displaying a parallel spring and damping virtual environment. The suggested absolute stable condition meets well with what is already generally accepted when the transmission stiffness trends to be infinite. Lastly the PHANToMDesktop is equivalent to be one-DOF on the manipulating space, and method for analyzing the stability and dynamic isotropy of analogous multi-DOF device is provided. Experimental results based on PHANToMDesktop show that the transmission stiffness has large effect on system stability.**

***Keywords*—haptic display, port theory, stability, virtual environment, transmission stiffness**

I. INTRODUCTION

Haptic display system in virtual reality includes three important parts: human manipulator, haptic device and virtual environment. Human manipulator acts on virtual reality and feels it through haptic device.

In a haptic display system, the haptic device is always regarded to be rigid ([1-3]), while ignoring the transmission stiffness. Considering a representative parallel spring and damping virtual environment, Colgate ever investigates the stability of a one-DOF haptic display system, and points out that the inherent damping exerts an overwhelming influence on the system stability([2,6]). Further more, this paper will take the transmission stiffness into account to investigate the stability of a haptic display system.

In section 2, the stability of a one-DOF haptic display system will be analyzed considering the effect of transmission stiffness. In section 3, mechanism of the last two links of PHANToMDesktop is equivalent to be one-DOF on the manipulating space to analyze its stability and isotropy, along with some experiments to support it. Section 4 is conclusion.

II. STABILITY ANLYSIS OF A ONE-DOF HAPTIC DISPLAY SYSTEM

A. Equivalent Electric Network of a One-DOF Haptic Display

A haptic display system is as shown in Fig.1. The human manipulator interacts with the virtual environment through haptic device. There are two kinds of information flowing modes as impedance display and admittance display, among which impedance display is more general. In an impedance display system the motion on the driving point of human manipulator is sampled as input information to the virtual environment, and the haptic device will display the force information computed from the virtual environment to the human manipulator.

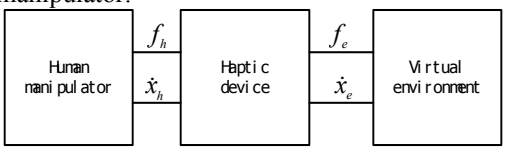

Figure 1. Elements in a Haptic Display System

A one-DOF haptic device is ever regarded as a rigid model of mass and damping. Here the transmission stiffness existing on the joint will be considered to investigate its effect on the system stability. As shown in Fig.2 is the model of a one-DOF haptic device, assuming that the mass of link manipulated by the human manipulator is m_l, the mass and damping of motor are m_m and b_m; the transmission stiffness between m_l and m_m is k_{tr}. In addition, the force and velocity on the driving point of human manipulator are f_h and $\dot{x}_h$; the force and velocity on the driving point of motor are f_m and $\dot{x}_m$. The force command to the haptic device is computed from virtual environment.

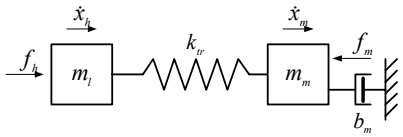

Figure 2. Model of a One-DOF Haptic Device

The dynamic equation of the haptic device is

$$f_h(s)=\left[m_l s+\frac{k_{tr}(m_m s+b_m)}{m_m s^2+b_m s+k_{tr}}\right]\dot{x}_h(s)+\frac{k_{tr}}{m_m s^2+b_m s+k_{tr}}f_m(s) \quad (1)$$

Where s is the Laplace operator.

As a general methodical tool in the area of virtual reality ([1,5]), here the electric network theory will be used to the stable analysis of a haptic display system considering transmission stiffness. A one-DOF haptic display system can be equivalent to an electric network as shown in Fig.3.

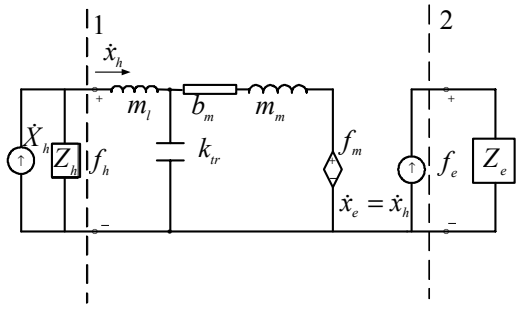

Figure 3. Equivalent Electric Network

In Fig.3, the left of broken line 1 is the model of human manipulator, which is a parallel of current origin $\dot{X}_h$ and passive impedance Z_h. $\dot{X}_h$ acts as the only input to the system. The right of broken line 2 is the model of passive virtual environment. The network between broken line 1 and 2 is the two-port connecting human manipulator and virtual environment. Assume that the virtual environment is a parallel spring and damping with passive impedance $Z_e=\frac{K_e}{s}+B_e$, where K_e and B_e are virtual stiffness and damping. The velocity $\dot{x}_h$ on the driving point of human manipulator acts as input information to the virtual environment, which can be expressed as

$$\dot{x}_e=\dot{x}_h \quad (2)$$

The force information computed from the virtual environment acts as control command to the haptic device. Also considering that the ZOH (zero-order hold) will lead to phase lag, the force information input to the haptic device is

$$f_m=G_{ZOH}f_e \quad (3)$$

Represent expression (2) and (3) to expression (1), then the impedance on the driving point of human manipulator is

$$Z_{eq}=\frac{f_h}{\dot{x}_h}=m_l s+\frac{k_{tr}(m_m s+b_m)}{m_m s^2+b_m s+k_{tr}}+\frac{k_{tr}}{m_m s^2+b_m s+k_{tr}}Z_e G_{ZOH} \quad (4)$$

The equivalent admittance is

$$Y_{eq}=\frac{\dot{x}_h}{f_h}=\frac{1}{Z_{eq}} \quad (5)$$

Where

$$G_{ZOH}=\frac{1-e^{-Ts}}{s}\approx\frac{2}{2+sT} \quad (6)$$

Where T is the sampling period of motion information on the human manipulator driving point.

B. Two-port Stable Theory

For an arbitrary two-port system, assume that its immittance matrix is

$$\begin{bmatrix}p_{11} & p_{12}\\ p_{21} & p_{22}\end{bmatrix} \quad (7)$$

Possible immittance matrixes are impedance matrix, admittance matrix and hybrid matrix. The sufficient and necessary condition for its absolute stability is ([1]):

$$\begin{cases}\mathrm{Re}(p_{11})\ge 0 \;\&\; \mathrm{Re}(p_{22})\ge 0\\ 2\,\mathrm{Re}(p_{11})\mathrm{Re}(p_{22})\ge |p_{12}p_{21}|+R_e(p_{12}p_{21})\end{cases}\forall\,\omega\ge 0 \quad (8)$$

Where $\mathrm{Re}(p_{ij})$ represents the real part of p_{ij}. Absolute stability means that a two-port system can keep stable whatever passive one-ports are connected to its two ports.

In a haptic display system, stability should be guaranteed when the human manipulator of arbitrary impedance interacts with the haptic device, which intends to display virtual environment with certain impedance model. The absolute stable condition for a two-port system provides a method to decide the range of some virtual environment parameters, within which the haptic display system will keep stable for any human manipulator impedance. As shown in expression (9) is the admittance equation of the haptic display system as Fig.3:

$$\begin{bmatrix}\dot{x}_h\\ \dot{x}_e\end{bmatrix}=\begin{bmatrix}Y_{eq} & 0\\ -Y_{eq} & 0\end{bmatrix}\begin{bmatrix}f_h\\ f_e\end{bmatrix} \quad (9)$$

According to expression (8) and (9), the absolute stable condition for the haptic display system under arbitrary human manipulator impedance is

$$\mathrm{Re}(Y_{eq})\ge 0 \quad (10)$$

Expression (10) provides the sufficient and necessary condition for the haptic display system under arbitrary human manipulator impedance.

C. Stable Analysis Considering Transmission Stiffness

For a virtual environment of parallel spring and damping, the stability will be evaluated by the achievable virtual spring rigidity to guarantee system stability.

According to expression (5) and (10), the absolute stable condition for a one-DOF haptic display system under arbitrary human manipulator impedance is:

$$2K_e\left[\left(k_{tr}-m_m\omega^2\right)T+2b_m\right] \le k_{tr}b_m\left(4+T^2\omega^2\right)+2B_e\left[2\left(k_{tr}-m_m\omega^2\right)-b_mT\omega^2\right] \quad \forall\omega\in[0,\infty) \tag{11}$$

Observing the left of expression (11), if $\left(k_{tr}-m_m\omega^2\right)T+2b_m=0$, there is

$$\omega_0=\sqrt{\frac{k_{tr}T+2b_m}{m_mT}} \tag{12}$$

To guarantee absolute stability of the system on $\omega=\omega_0$, the right of expression (11) should be constantly greater than zero on $\omega=\omega_0$. To satisfy this condition, there is

$$k_{tr}>\frac{2B_e}{T} \tag{13}$$

If the transmission stiffness doesn't satisfy expression (13), the absolute stability can't be realized for any virtual spring rigidity. If expression (13) is satisfied, it can be deduced from expression (11) that the achievable virtual spring rigidity to guarantee absolute stability when $\left(k_{tr}-m_m\omega^2\right)T+2b_m\neq 0$ is

$$\begin{cases} K_e\le\dfrac{k_{tr}b_m\left(4+T^2\omega^2\right)+2B_e\left[2\left(k_{tr}-m_m\omega^2\right)-b_mT\omega^2\right]}{2\left[\left(k_{tr}-m_m\omega^2\right)T+2b_m\right]} \\ \qquad if\left(k_{tr}-m_m\omega^2\right)T+2b_m>0 \\ K_e\ge\dfrac{k_{tr}b_m\left(4+T^2\omega^2\right)+2B_e\left[2\left(k_{tr}-m_m\omega^2\right)-b_mT\omega^2\right]}{2\left[\left(k_{tr}-m_m\omega^2\right)T+2b_m\right]} \\ \qquad if\left(k_{tr}-m_m\omega^2\right)T+2b_m<0 \end{cases} \tag{14}$$

For any value of ω except ω_0, expression (14) is equivalent to

$$\begin{cases} K_e\le\dfrac{2k_{tr}\left(b_m+B_e\right)}{k_{tr}+2b_m} & decided\ by\ \omega\to 0 \\ K_e\ge\dfrac{4m_mB_e+2B_eb_mT-k_{tr}b_mT^2}{2m_mT} & decided\ by\ \omega\to\infty \end{cases} \tag{15}$$

Expression (15) can be simplified as

$$\frac{4m_mB_e+2B_eb_mT-k_{tr}b_mT^2}{2m_mT}\le K_e\le\frac{2k_{tr}\left(b_m+B_e\right)}{k_{tr}T+2b_m} \tag{16}$$

So expression (13) and (16) provide the absolute stable condition for a haptic system displaying a virtual parallel spring and damping. When $k_{tr}\to\infty$, expression tends to be

$$K_e\le\frac{2\left(b_m+B_e\right)}{T} \tag{17}$$

Expression (17) meets well with the accepted result ([6]) when transmission stiffness is ignored, which illuminates that expression (16) is more general.

III. EXPERIMENTAL STUDY BASED ON PHANTOMDESKTOP

PHANToM is a series of commercial haptic devices. A pure spring virtual environment as a special case of parallel spring and damping is displayed through PHANToMDesktop in this experiment, and the effect of transmission stiffness on system stability will be approximately evaluated.

A. PHANToMDesktop and its Jacobin Matrix

As shown in Fig.4 is the photo and mechanism of PHANToMDesktop. Considering convenience of analysis and assuming that link 2 and 3 are at the same plane, the system stability is examined on the plane decided by the second and third links. Establish coordinate on this plane: the origin is on center of the second joint; the y axis is on the same direction as the first joint axis; the z axis is perpendicular to the first joint axis. The length of link 2 and 3 are l_2 and l_3. Assume that the home position is on where link 2 parallel to z axis and link 3 perpendicular to link 2, θ_2 and θ_3 respectively are the anti-clockwise angular displacement of joint 2 and 3 from the home position. Velocity on the end-effector is $\left[\dot z\quad \dot y\right]^T=J\left[\dot\theta_2\quad \dot\theta_3\right]^T$, where $\left[\dot\theta_2\quad \dot\theta_3\right]^T$ is the angular velocity vector of joint 2 and 3, J is the Jacobin matrix:

$$J=\begin{bmatrix} -l_2\sin\theta_2+l_3\cos(\theta_2+\theta_3) & l_3\cos(\theta_2+\theta_3) \\ l_2\cos\theta_2+l_3\sin(\theta_2+\theta_3) & l_3\sin(\theta_2+\theta_3) \end{bmatrix} \tag{18}$$

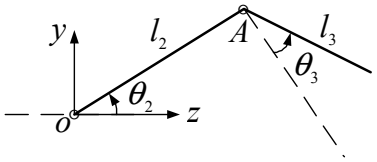

a. Photo of PHANToMDesktop b. Mechansim

Figure 4. Photo and Mechanism of PHANToMDesktop

B. Damping and Transmission Stiffness of PHANToMDesktop

PHANToMDesktop is cable-transmissioned, and the cable is twisted directly on output shaft of the motor. The rotational damping of the second and third motor can be computed as:

$$b_{ri}=\frac{I_{mi}}{T_{mi}},\quad i=2,3 \tag{19}$$

Where I_{mi} and T_{mi} is the rotor inertia and mechanical time constant of motor 2 and 3. Assuming that the rotational speed of the second and third motors are $\dot\theta_{mi}$, $i=2,3$, τ_{mi} is needed to conquer the motor damping.

$$\tau_{mi} = b_{ri}\dot{\theta}_{mi}, \quad i = 2,3 \tag{20}$$

Assuming that there is no slip, the translational speed of the cable twisted on each motor is

$$v_i = r_{mi}\dot{\theta}_{mi}, i = 2,3 \tag{21}$$

Where r_{mi} is the output radius of motor 2 and 3. The equivalent translational damping on the motor is b_{ti}, $i = 2,3$, to conquer which the tangential force on the cable should be:

$$f_i = \tau_{mi} r_{mi} = b_{ti} v_i, \; i = 2,3 \tag{22}$$

Integrate expression (19)—(22), the equivalent translational damping on the output radius of motor 2 and 3 is

$$b_{ti} = \frac{I_{mi}}{T_{mi} r_{mi}^{\;2}}, \quad i = 2,3 \tag{23}$$

Assuming that the joint flexibility is centralized on the cable transmission, the transmission stiffness can be computed as ([7,8]):

$$k_{tr} = \frac{NEA}{L} \tag{24}$$

In expression (24), N and L respectively are the transmission ratio and transmission length, E and A respectively are the elastic ratio and sectional area of the cable. Observation shows that there are respectively one-level and two-level cable transmission on joint 2 and 3. The transmission stiffness k_{tr2} on joint 2 can be directly computed from (24). Assuming that the stiffness of the first and second transmission level of joint 3 respectively is k_{tr31} and k_{tr32}, which can be computed from expression (24), then the transmission stiffness on joint 3 can be approximately computed from $k_{tr3} = \dfrac{k_{tr31} k_{tr32}}{k_{tr31} + k_{tr32}}$.

C. *One-DOF Equivalence and Stability Analysis*

On an arbitrary position and orientation of the manipulating workspace, the last two joints of PHANToMDesktop will be equivalent to be one-DOF as shown in Fig.2. m_m and m_l respectively is the equivalent moving mass of motors and links, which is computed in ([9]); b_m and k_{tr} is the equivalent one-DOF damping and transmission stiffness; f_h and $\dot{x}_h$ respectively is the force and velocity on the driving point of human manipulator; f_m and $\dot{x}_m$ respectively is the force and velocity on m_m. From (16), if the virtual environment is pure spring or a virtual wall as $Z_e = \dfrac{K_e}{s}$, the range of achievable virtual spring rigidity is:

$$K_e \le \frac{2k_{tr}b_m}{k_{tr}T + 2b_m} \tag{25}$$

The following will provide the equivalent one-DOF damping and stiffness of the two-DOF haptic mechanism.

Assuming R_2 and R_3 are the final output radius of joint 2 and 3, the equivalent rotational damping of each motor on joint 2 and joint 3 respectively are

$$b_2 = b_{t2} R_2^{\;2}, \; b_3 = b_{t3} R_3^{\;2} \tag{26}$$

To conquer motor damping the joint torque should be

$$\tau_{bi} = b_i \dot{\theta}_i, \quad i = 2,3 \tag{27}$$

The equivalent rotational transmission stiffness on joint 2 and 3 respectively is

$$k_2 = k_{tr2} R_2^{\;2}, \; k_3 = k_{tr3} R_{32}^{\;2} \tag{28}$$

Assuming the distortion on each joint are $\Delta\theta_{d2}$ and $\Delta\theta_{d3}$, joint torque generating such a distortion should be

$$\tau_{ki} = k_i \Delta\theta_{di}, \quad i = 2,3 \tag{29}$$

Assuming that end-effector velocity on the manipulating space is v_e, and force needed to conquer the motor damping is f_b; also assuming that the distortion because of transmission stiffness on the manipulating space is Δd_e, and force needed to generate such a distortion is f_k, then

$$\tau_b = J^T f_b = D\dot{\theta} \tag{30}$$

$$\tau_k = J^T f_k = K\Delta\theta_d \tag{31}$$

Where D and K respectively are the damping and stiffness matrix on joint space.

$$D = \begin{bmatrix} b_2 & 0 \\ 0 & b_3 \end{bmatrix}, \; \dot{\theta} = \begin{bmatrix} \dot{\theta}_2 & \dot{\theta}_3 \end{bmatrix}^T \tag{32}$$

$$K = \begin{bmatrix} k_2 & 0 \\ 0 & k_3 \end{bmatrix}, \; \Delta\theta_d = \begin{bmatrix} \Delta\theta_{d2} & \Delta\theta_{d3} \end{bmatrix}^T \tag{33}$$

Represent $\dot{\theta} = J^{-1} v_e$ and $\Delta\theta_d = J^{-1}\Delta d_e$ to expression (30) and (31), there is

$$f_b = J^{-T} D J^{-1} v_e \tag{34}$$

$$f_k = J^{-T} K J^{-1} \Delta d_e \tag{35}$$

From expression (34) and (35), the damping and stiffness matrix on a certain position of the manipulating space respectively is

$$b_w = J^{-T} D J^{-1} \tag{36}$$

$$k_w = J^{-T} K J^{-1} \tag{37}$$

Assuming that the slope angle between normal of the virtual wall and z axis on plane yoz is γ, and end-effector velocity and distortion on the direction respectively are

$v_e = \begin{bmatrix} \dot{z} & \dot{y} \end{bmatrix} = |v_e| \begin{bmatrix} \cos\gamma & \sin\gamma \end{bmatrix}^T$ and

$\Delta d_e = \begin{bmatrix} \Delta z & \Delta y \end{bmatrix} = |\Delta d_e| \begin{bmatrix} \cos\gamma & \sin\gamma \end{bmatrix}^T$, where $|v_e|$ and $|\Delta d_e|$ respectively is the modulo of velocity and distortion, from expression (34) and (35), the square of $|f_b|$ and $|f_k|$ is

$$|f_b|^2 = f_b{}^T f_b = v_e{}^T b_w{}^T b_w v_e \quad (38)$$

$$|f_k|^2 = f_k{}^T f_k = \Delta d_e{}^T k_w{}^T k_w \Delta d_e \quad (39)$$

According to expression (18) and (32)—(39), the equivalent damping and stiffness b_m and k_{tr} on certain position and orientation can be completely solved out.

Each position on the manipulating space can be characterized by joint displacement. Take point $(45^\circ, -45^\circ)$ as an example to analyze the stability and isotropy. Approximate measurement shows $l_2 = 150mm$ and $l_3 = 100mm$. The Jacobin matrix on this point is

$$J|_{(45^\circ,-45^\circ)} = \begin{bmatrix} -0.006m & 0.1m \\ 0.106m & 0 \end{bmatrix} \quad (40)$$

From expression (32), (33), (36), (37) and (40), the damping and stiffness matrix on the manipulating space at $(45^\circ, -45^\circ)$ approximately is

$$b_w|_{(45^\circ,-45^\circ)} = \begin{bmatrix} \dfrac{b_3}{J_{21}|_{(45^\circ,-45^\circ)}{}^2} & 0 \\ 0 & \dfrac{b_2}{J_{12}|_{(45^\circ,-45^\circ)}{}^2} \end{bmatrix} \quad (41)$$

$$k_w|_{(45^\circ,-45^\circ)} = \begin{bmatrix} \dfrac{k_3}{J_{21}|_{(45^\circ,-45^\circ)}{}^2} & 0 \\ 0 & \dfrac{k_2}{J_{12}|_{(45^\circ,-45^\circ)}{}^2} \end{bmatrix} \quad (42)$$

According to expression (38)—(42), on an arbitrary angle γ at point $(45^\circ, -45^\circ)$, the equivalent damping and stiffness on the manipulating space is

$$b_m = \frac{|f_b|}{|v_e|} = \sqrt{\left(\frac{b_3 \cos\gamma}{J_{21}|_{(45^\circ,-45^\circ)}{}^2}\right)^2 + \left(\frac{b_2 \sin\gamma}{J_{12}|_{(45^\circ,-45^\circ)}{}^2}\right)^2} \quad (43)$$

$$k_{tr} = \frac{|f_k|}{|\Delta d_e|} = \sqrt{\left(\frac{k_3 \cos\gamma}{J_{21}|_{(45^\circ,-45^\circ)}{}^2}\right)^2 + \left(\frac{k_2 \sin\gamma}{J_{12}|_{(45^\circ,-45^\circ)}{}^2}\right)^2} \quad (44)$$

Then the achievable spring rigidity can be computed from (25) if any design parameters are known to us.

Through observation, estimate that the two motors on the last two joints of PHANToMDesktop are both MaxonRE26 or approximate series, and the output radius is $r_{mi} = 2mm, i = 2,3$. Approximate measurement shows that $R_2 = 30mm$ and $R_3 = 15mm$. The motor manual shows that the parameters of MaxonRE26-118774 are $I_m = 11.6gcm^2$ and $T_m = 5ms$ .according to (23), there is $b_{t2} = b_{t3} = \dfrac{I_m}{T_m r_{mi}{}^2} = 58N \cdot sec/m$. To obviate serious uncertainty, the transmission stiffness will not be estimated, and the achievable spring rigidity of PHANToMDesktop will be approximately computed according to the accepted principle as expression (17) based on rigid model. Sampling period of the system is $T = 1ms$. According to expression (26) and (43), on orientation of $\gamma = 90^\circ, 60^\circ, 30^\circ, 0^\circ$ at point $(45^\circ, -45^\circ)$, the equivalent damping and achievable spring rigidity when ignoring transmission stiffness are shown in Table 1, where $K_{e\max}$ is the maximum of achievable spring rigidity. The following will check if the expected $K_{e\max}$ based on rigid model can be reached in actual experiment.

TABLE 1. EQUIVALENT dAMPING AND ACHIEVABLE SPRING STIFFNESS ON EACH ORIENTATION AT $(45^\circ, -45^\circ)$

	$\gamma = 90^\circ$	$\gamma = 60^\circ$	$\gamma = 30^\circ$	$\gamma = 0^\circ$
$b_m(N\sec/m)$	5.22	4.97	2.64	1.31
$K_{e\max}(KN/m)$	10.44	9.94	5.28	2.62

D. Experiment and Result Analysis

Intention of this experiment is to measure the actual achievable spring rigidity at point $(45^\circ, -45^\circ)$, and testify that there must be other factors except motor damping affecting the system stability, especially transmission stiffness.

Establish virtual spring or virtual wall $Z_e = \dfrac{K_e}{s}$ with normal on plane yoz and starting from point $(45^\circ, -45^\circ)$. On each orientation of $\gamma = 90^\circ, 60^\circ, 30^\circ, 0^\circ$ at $(45^\circ, -45^\circ)$, increase the spring rigidity gradually to find out the largest achievable rigidity for the two-DOF haptic display system of PHANToMDesktop. During the experiment, the human manipulator should keep a constant manner, and always try to extrude the virtual wall. The experimental phenomena and result analysis are as the following.

1. On $\gamma = 90^\circ$. Fig.5 is a series of curves of embed-depth on virtual wall vs. time along with the virtual spring rigidity varying from $1.5KN/m$ to $6KN/m$. When the rigidity is small the curve is relatively smooth, fluctuation of little amplitude is due to the natural response of human manipulator to force, which doesn't affect stability of the system. The system instability becomes obvious when $K_e = 5.5KN/m$. And the system becomes completely unstable and start to oscillate when $K_e = 6KN/m$, where the human manipulator can't feel any force.

2. On $\gamma = 60^\circ$. Fig.6 is a series of curves of embed-depth vs. time from $4.5KN/m$ to $6KN/m$. When $K_e = 6KN/m$, the haptic display system comes to be obviously unstable.
3. On $\gamma = 30^\circ$. Fig.7 is a series of curves from $1KN/m$ to $2.5KN/m$. On this direction, the achievable spring rigidity is evidently decreased to be $K_e = 2.5KN/m$.
4. On $\gamma = 0^\circ$. Fig.8 is a series of curves from $0.5KN/m$ to $1.5KN/m$. The achievable spring rigidity is steeply decreased to be $K_e = 1.5KN/m$.

As summarization, at point $(45^\circ, -45^\circ)$ on the manipulating space, along with the decrease of γ, the stability of the system will decrease. As seen from Table 1, if the transmission stiffness is ignored the achievable spring rigidity can be as large as $10KN/m$, but experiment shows that the actual limit is $6KN/m$. So, as shown in expression (16), it can be predicated that the effect of transmission stiffness on the system stability can't be ignored. Complete estimation and experiment based on the above analysis considering transmission stiffness can be seen in ([9]).

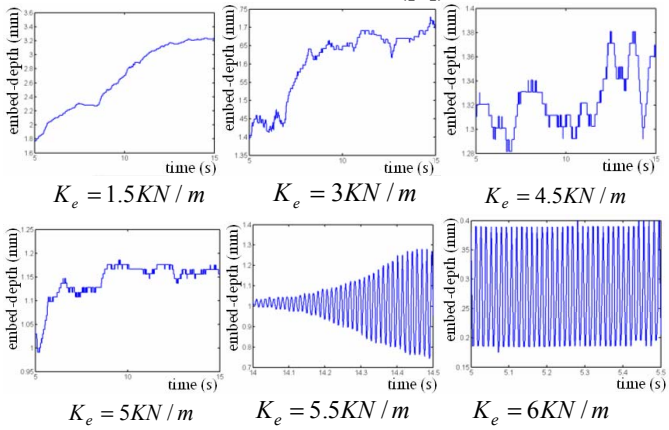

Figure 5. Embed-depth on Virtual Wall vs. Time on $\gamma = 90^\circ$

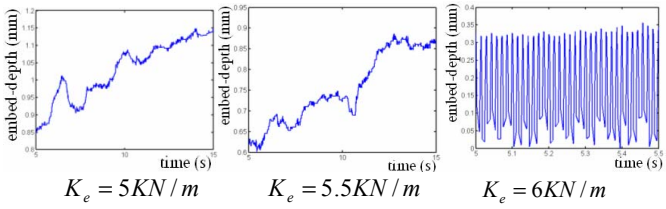

Figure 6. Embed-depth on Virtual Wall vs. Time on $\gamma = 60^\circ$

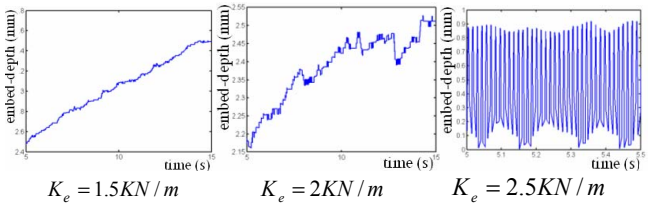

Figure 7. Embed-depth on Virtual Wall vs. Time on $\gamma = 30^\circ$

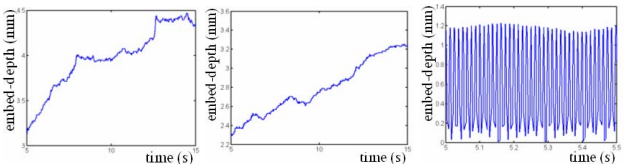

Figure 8. Embed-depth on Virtual Wall vs. Time on $\gamma = 0^\circ$

IV. CONCLUSION

The effect of transmission stiffness on a haptic display system is quantitatively investigated. The analysis can be proved to be reasonable because it meet well with an accepted opinion when the transmission stiffness inclines to be infinite. Mechanism of the last two joints of PHANToMDesktop is equivalent to be one-DOF to examine its stability, and experimental results further prove the effect of transmission stiffness. If the parameter of an analogous multi-DOF haptic device is knowable, stability of the haptic displace system can be approximately evaluated based on the suggested one-DOF equivalent method and absolute stable condition.

REFERENCE

[1] Adams R J, Hannaford B. Stable Haptic Interaction with Virtual Environments[J]. IEEE Transactions on Robotics and Automation, 1999，15(3): 465-474

[2] Colgate J E, Schenkel G, Passivity of a Class of Sampled-Data Systems: Application to Haptic Interfaces[A]. In: Proc. Of the American Control Conference[C]. Baltimore, Maryland: 1994. 3236-3240

[3] Daniel R W, McAree P R. Fundamental Limits of Performance for Force Reflecting Teleoperation[J]. the International Journal of Robotics Research, 1998，17(8):811-830

[4] Luo Yangyu, Wang Dangxiao, Zhang Yuru, Development of a Haptic Display Interface[A]. In: 2nd International Symposium on Instrumentation Science and Technology[C]. Jinan, China: 2002. 272-276

[5] Hannaford B, A Design Framework for Teleoperators with Kinesthetic Feedback[J]. IEEE Transactions on Robotics and Automation, 1989, 5(4): 426-434

[6] J. Edward Colgate and J. Michael Brown, "Factors Affecting the Z-Width of a Haptic Display," Proc. Of the IEEE Int. Conf. On Robotics and Automation, pp. 3205-3210, 1994

[7] Townsend, W.T., Salisbury, J.K., Mechanical Bandwidth as a guideline to High-Performance Manipulator Design, IEEE Proceedings. of the International Conference on Robotics and Automation, 1989, pp. 1390-1395

[8] Townsend, W.T., The Effect of Transmission Design on Force-Controlled Manipulator Performance, Doctoral dissertation, Mechanical Engineering, Massachusetts Institute of Technology, 1988

[9] Luo Yangyu, Performance Analysis and Designing Method of Haptic systems Doctoral dissertation，Beijing University of Aeronautics and Austronautics，Beijing, China, 2003 (in Chinese)